Key Engineering Materials
ISSN: 1662-9795, Vol. 926, pp 499-510
doi:10.4028/p-g4wbpz

Submitted: 2021-12-21
Revised: 2022-03-01
Accepted: 2022-03-01
Online: 2022-07-22

Copper Wire Multi-Pass Drawing: Process Modeling and Optimization

Sara Di Donato[1,a*], Lorenzo Donati[1,b] and Marco Negozio[1,c]

[1*]DIN-Department of Industrial Engineering, University of Bologna, Viale Risorgimento 2, 40136, Bologna, Italy

[a]sara.didonato2@unibo.it, [b]l.donati@unibo.it, [c]marco.negozio2@unibo.it

Keywords: multi-pass wire drawing, copper, drawing tension, back tension, capstan

Abstract. During cold wire drawing process, the drawing stress applied to the wire at the exit of the die must be lower than the material yield stress (including strain-hardening) to avoid wire necking and fracture. Several studies have been developed to investigate and model the stress acting on the wire in the single pass drawing and its dependence on the main process parameters. The aim of this work is to apply an analytical model for the calculation of the drawing stresses during the whole complex multi-pass manufacturing process in industrial environment, considering not only the forces acting in the die but also the driving forces of the rotating capstans (drawing tension and back tension). The drawing of ETP Pure Copper (99.9% in weight), using two industrial multi-pass machines with different reduction ratio sequences, is analysed and then discussed in order to understand the different failure rates. Finally, the study compared step by step, the evolution of the drawing stresses respect to material yield stress when different processing conditions (i.e. change of capstan windings, change of friction conditions in the die and in the capstan) are applied.

Introduction

The drawing technology is a cold metal forming process that is mainly used for the production of wires, bars or tubes. In wire drawing technology, the process consists in reducing the cross-section of the starting rod, through its deformation inside several dies with decreasing diameter. This deformation is produced by the application of a traction force at the exit of the die. Such pull force creates a triaxial stress state in the die able to permanently reduce the diameter of the wire and consequently strain hardened the material due to the large deformation in the cold working process. Therefore, one of the main limitations of the process is given by the need to keep the pull stress always below the yield stress of the material (strain hardening included), thus avoiding necking and wire breaks. This condition limits the wire reduction of a single pass, so that multi-passes are needed in order to achieve the requested final dimensions. Nowadays the process is carried out continuously using complex industrial multi-steps machines characterized by high deformation rates.

Several models have been proposed in the literature for the analytical computation of the material deformation process during wire drawing. The slab method, firstly proposed by Siebel [1],[2],[3], is one of the most widespread in relation to its simple application. It involves the definition of the equilibrium forces by dividing the whole section area of the wire in smaller parts (slab) and then integrating the equation in the drawing direction. The method employs the assumption of homogenous deformation field along the slab height with the normal stress uniformly distributed on the plane parallel to it; the integral equation's solution results from these simplified boundary conditions. Another analytical method was developed by Wistreich [4] and then applied by Wright [5]: it involves the evaluation of a ‘deformation zone shape parameter’ depending on the reduction ratio and the die's semi-angle; the contribution of the distortion and friction works are calculated by introducing a redundant work factor obtained with semi-empirical approaches from physical measurements and depending on the deformation zone shape parameter. Owing to the complexity of the equations, the values of the factor are available only in tabular or graphical form. In both theories (Wistreich and Siebel), the additional friction work due to the presence of the bearing length downstream of the drawing cone is omitted. One of the most notable model was proposed by Avitzur [6],[7]: it involves the application of the Upper-Bound approach to the drawing problem, dividing the wire into three zones, in each of which the velocity field is assumed to be continuous. The inlet and

exit zones of the die are characterized by the lack of deformation in the wire and the axial component of the velocity is uniform, while in the central zone the plastic flow occurs and the velocity field is directed toward the cone's apex with axial cylindrical symmetry. Avitzur's method involves the friction work due to the presence of the bearing length.

It is known that the wire drawing process depends on three main parameters: the wire material properties, the die geometry (such as die angle and reduction ratio) and the process conditions (such as friction at the interface between the die and the wire). Over the years, several researchers focused their attention on investigating the influence of these parameters on the process. Dixit and Dixit [8] studied the effect of the reduction ratio, the die semi-angle, the friction coefficient and the back tension on die pressures and on the pull stress. They found that an increase in the reduction, or a decrease in the die angle, or a decrease of the friction coefficient tends to homogenize the wire deformation over the cross section. Otherwise, with low reduction and large die-angle, the plastic zone near the axis of symmetry narrows down and may eventually disappear, causing the central bursting defect to occur. Vega et al. [9] applied the Avitzur's model and investigated the effects of the die angle, the friction coefficient and the reduction ratio on the drawing force during the copper wire drawing process. They showed that the drawing force increases when the reduction ratio and the die angle increase, while the friction coefficient affects the optimum die angle value corresponding to the minimum value of the drawing force: the optimum die angle increases with increasing coefficient of friction. M. Tintelecan et al. [10] carried out an experimental campaign to calculate the value of the drawing force using dies with different semi-angles and bearing lengths and to estimate their optimal values for steel wire drawing. They obtained the smallest values for experimental drawing force with the die semi-angle between 6° and 8° and the bearing length corresponding to 40% of the final diameter. An estimation of the friction coefficient between wire and die was attempted by A.I. Obi et al. [11], by measuring drawing stress and applying Avitzur's model on a drawing single step, using a hydraulic machine. They tested the potential of some fatty-based oils as lubricants for steel and copper drawing operations from the coefficient of friction obtained during the material flow through conical converging dies. Lazzarotto et al. [12] proposed a method to evaluate the friction coefficient based on the upsetting sliding test. They applied the method to evaluate the coefficient of friction between material and die during the wire drawing process of a phosphate stearate coated 1035 steel. The experiment was validated through finite element analysis and it was proved that the test can be a good tool for the identification of Coulomb's friction coefficient in actual conditions of wire drawing process. A. Haddi et al. [13] studied the relation between the friction coefficient and the temperature, showing that the drawing stress and temperature evolve during the drawing process, because of the variation of the friction coefficient. They carried out an experimental test on a single pass copper wire drawing, showing that the drawing stress and the temperature increase rapidly at the start of the test, for the drawing speed from 0 to 1 m/s; then the flow stress value varies from 300 MPa (reference value for a quasi-static tensile test) to 430 MPa for wire drawing speed of 7 m/s and the temperature increases from 50 °C to 68 °C. Therefore, they found that the friction coefficient and flow stress depend on temperature and strain rate respectively and with these assumptions provided a modification of the formulation proposed by Avitzur. G.A.S. Martinez et al. [14] carried out an investigation on the operational parameters to obtain the best combination that minimizes the energy consumption during the process. The effects of the drawing speed, drawing force, temperature and tension distribution on the wire drawing were investigated using an experimental and numerical approach. They found that the dies with die angle of 18° reach the minimal friction coefficients at the most significant speed (20.6-24.2 m/s); instead, those with die angles of 14° reach the minima at smaller speeds (14.4-18.7 m/s), due to the difference in dragging the lubricant associated with the different geometries of the dies. The temperature of the process depends on the initial temperature of the material, die geometry, type of lubricant, and heat generated by the deformation of the material. Compressive stresses on the surface and at the centre of the wire are larger for dies with larger die angles; on the other hand, dies with a smaller die angle show a more homogenous as far as to the distribution of radial stresses is concerned.

In the previously discussed papers, the efforts made in the research for the optimization of the process have always been focused on the single wire-drawing pass. In the multi-pass industrial machines, the deformation is achieved continuously and at the same time on several dies. Between two consecutive dies, rotating capstans pulls the wire thus generating the pull force but also a back force. Indeed, the capstan speed is greater than the speed of the wire wrapped around it, thus generating slip and, consequently, transmitting pull and back tension to the wire. To the best of the authors' knowledge, only J. Thimont et al. [15] introduced a modeling that considered pull forces by capstans and die pressure in the multi-pass drawing process. They investigated the wire drawing process performed by ArcelorMittal WireSolutions to produce high strength steel wire. After developing a constitutive law based on the wire microstructure evolution, they developed a multi-pass drawing theoretical model applied to an industrial machine consisting of 14 passes of wire reduction, considering the relation between drawing force and back-pull force. Nevertheless, further investigations for the development of a reliable analytical model are still needed.

In this work, a theoretical multi-pass wire drawing model considering the whole process was developed, focusing on the relation between drawing stress and back-stress, following Aviztur model. The model was applied to ETP Pure Copper (99.9% in weight) wire drawing performed with two different commercial industrial machines. The drawing stresses acting on the material were investigated considering the variation of process parameters such as the friction coefficient between wire and die, between wire and capstan and the number of wire windings around the capstans.

Experimental Trials

The wire drawing process was performed on ETP Pure Copper (99.9% in weight) at the ICEL s.c.p.a company of Lugo (Italy). The wire rod was subjected to a preliminary drawing process from a diameter of 8.00 mm to 1.83 mm (area reduction 94.77%). Subsequently, without any annealing treatment, 21 drawing passes were carried out up to a final diameter of 0.205 mm, which corresponds to a total strain of $\bar{\varepsilon} = 7.33$ (total area reduction 99.93%). This value was calculated according to Eq. 1 [2]:

$$\bar{\varepsilon} = 2\ln\frac{D_i}{D_f}, \tag{1}$$

where D_i and D_f are the initial and final diameters.

The 21 drawing passes were carried out using two industrial multi-pass machines with different mechanical elongation ratios as summarized in Table 1. The two machines consist of 21 dies (drawing passes) and 20 capstans; at the outlet of the machine the wire enters directly into the annealer. Dies with semi-angle of 9° and bearing lengths of 25% of the final diameter are mounted on both machines (Fig. 1)

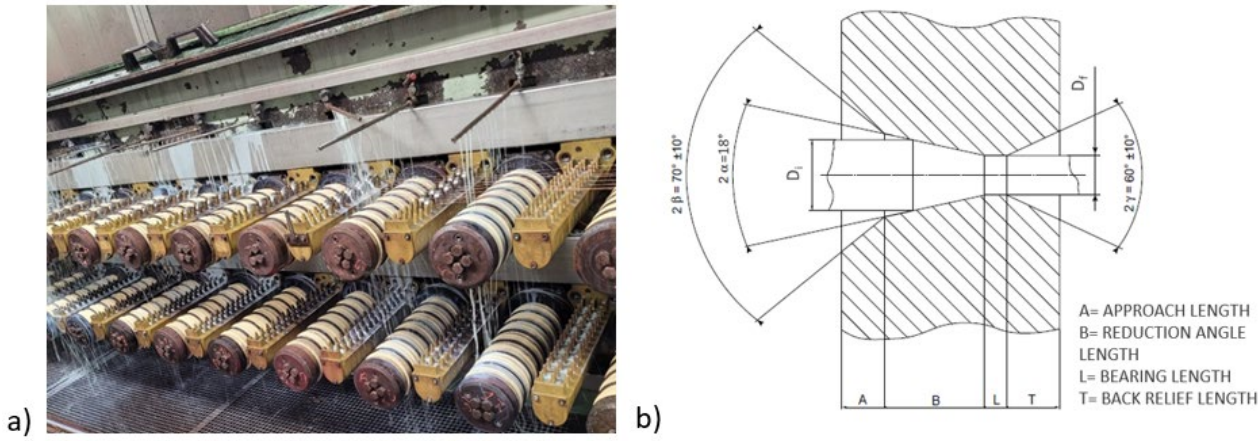

Fig. 1: a) Picture of industrial machine used in ICEL s.c.p.a. b) Diagram of the die (the profile of the die is not so sharp, as shown in the diagram, but the different areas are blended together with rounded edges).

Machine and wire elongation at each pass of reduction are calculated as follow (Eqs. 2-3): [16],[3]

$$E\%_{machine_i} = \left(\frac{S_{C_i}}{S_{C_{i-1}}} - 1\right) * 100\ , \tag{2}$$

$$E\%_{wire_i} = \left[\left(\frac{D_{i_i}}{D_{f_i}}\right)^2 - 1\right] * 100\ ; \tag{3}$$

where S_{C_i} is the tangential speed of the capstan, which is placed at the exit of the die, after the i-th pass of reduction from the initial diameter D_{i_i} to the final D_{f_i}.

Table 1 Comparison between the mechanical characteristics of Machine 1 and Machine 2.

	MACHINE N°1					MACHINE N°2				
N° Pass	**Diameter Initial** [mm]	**Diameter Final** [mm]	**Reduction Ratio** [%]	**Wire Elongation** [%]	**Machine Elongation** [%]	**Diameter Initial** [mm]	**Diameter Final** [mm]	**Reduction Ratio** [%]	**Wire Elongation** [%]	**Machine Elongation** [%]
1	1.83	1.592	24.3	32.1	24.0	1.830	1.6144	22.2	28.5	25.0
2	1.592	1.417	20.8	26.2	24.0	1.6144	1.4382	20.6	26.0	25.0
3	1.417	1.261	20.8	26.3	24.0	1.4382	1.2813	20.6	26.0	25.0
4	1.261	1.122	20.8	26.3	24.0	1.2813	1.1415	20.6	26.0	25.0
5	1.122	0.998	20.9	26.4	24.0	1.1415	1.0169	20.6	26.0	25.0
6	0.998	0.888	20.8	26.3	24.0	1.0169	0.9059	20.6	26.0	25.0
7	0.888	0.790	20.9	26.3	24.0	0.9059	0.8071	20.6	26.0	25.0
8	0.790	0.703	20.8	26.3	24.0	0.8071	0.719	20.6	26.0	25.0
9	0.703	0.626	20.7	26.1	24.0	0.719	0.6405	20.6	26.0	25.0
10	0.626	0.557	20.8	26.3	24.0	0.6405	0.5706	20.6	26.0	25.0
11	0.557	0.495	21.0	26.6	24.0	0.5706	0.5187	17.4	21.0	19.2
12	0.495	0.441	20.6	26.0	24.0	0.5187	0.4716	17.3	21.0	19.2
13	0.441	0.392	21.0	26.6	24.0	0.4716	0.4287	17.4	21.0	19.2
14	0.392	0.359	16.1	19.2	17.2	0.4287	0.3897	17.4	21.0	19.2
15	0.359	0.329	16.0	19.1	17.2	0.3897	0.3543	17.3	21.0	19.2
16	0.329	0.301	16.3	19.5	17.2	0.3543	0.3221	17.4	21.0	19.2
17	0.301	0.276	15.9	18.9	17.2	0.3221	0.2928	17.4	21.0	19.2
18	0.276	0.253	16.0	19.0	17.2	0.2928	0.2662	17.3	21.0	19.2
19	0.253	0.232	15.9	18.9	17.2	0.2662	0.242	17.4	21.0	19.2
20	0.232	0.213	15.7	18.6	17.2	0.242	0.22	17.4	21.0	19.2
21	0.213	0.205	7.4	8.0	-	0.22	0.205	13.2	15.2	-

It has to be noted that the machine elongation, which depends on the transmission ratio of the gears' train moving the capstans (Eq. 2), must be always lower than the wire elongation (Eq. 3) at each pass in order to work with a slip condition between the capstans and the wire.

Fig. 2 shows the data collected during the monitoring of the wire breaks that occurred within the two machines over a period of 60 days, divided into four time periods of 15 days each to carry out a statistical analysis of the failure rate of the machines. Machine 1 was found to have a higher failure rate than Machine 2, with a wire break occurring on average every 2.5 days compared with every 4 days on Machine 2.

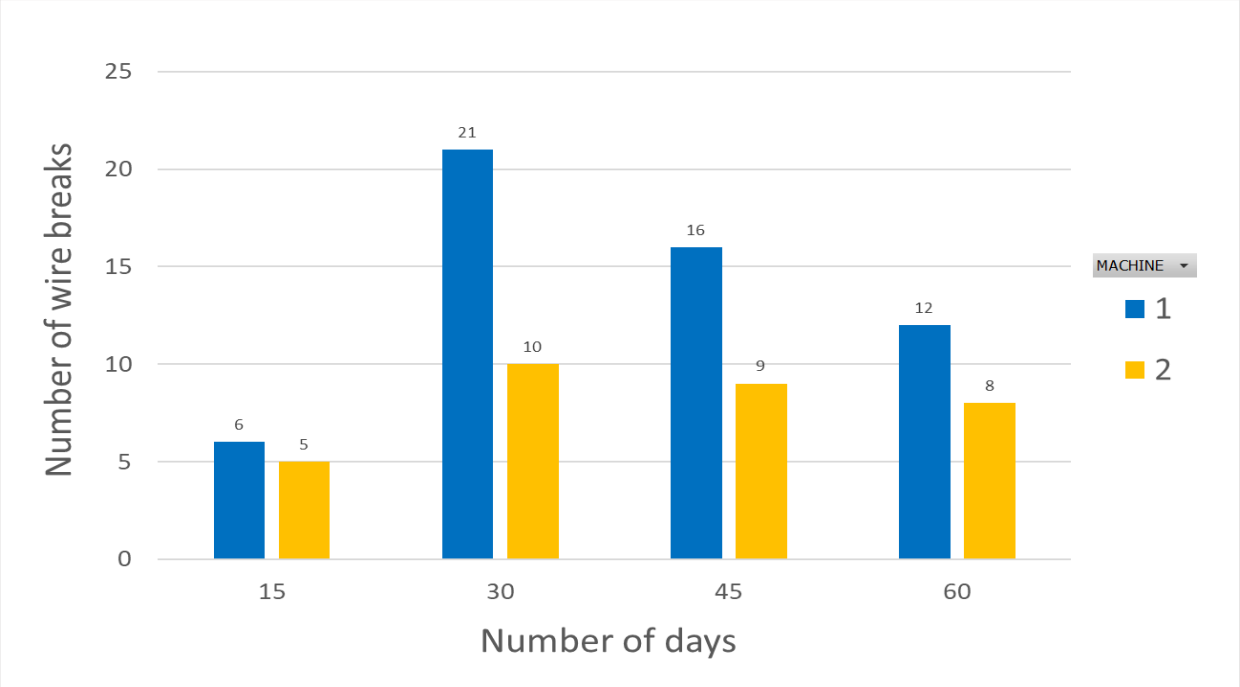

Fig. 2 Monitoring of the wire breaks that occurred on the two machines in 60 days, divided into four time periods of 15 days each.

Multi-Pass Implemented Model

Avitzur's theory [6],[7] has been used to model the multi-pass drawing process. This model involves the drawing stress calculation (Eq. 4) using the Coulomb friction coefficient μ acting between wire and die, and considering four energy components: deformation, distortion (redundant), friction and the contribution given by the presence of back tension at the inlet of the die:

$$\sigma_{d_i} = \overline{\sigma}_{m_i} \frac{\frac{\sigma_{b_i}}{\overline{\sigma}_{m_i}} + 2f(\alpha)\ln\left(\frac{R_{ii}}{R_{fi}}\right) + \frac{2}{\sqrt{3}}\left(\frac{\alpha}{sen^2(\alpha)} - \cot(\alpha)\right) + 2\mu\left[\cot(\alpha)\left(1 - \frac{\sigma_{bi}}{\overline{\sigma}_{m_i}} - \ln\left(\frac{R_{ii}}{R_{fi}}\right)\right)\ln\left(\frac{R_{ii}}{R_{fi}}\right) + \frac{L_i}{R_{fi}}\right]}{\left(1 + 2\mu\frac{L_i}{R_{fi}}\right)}, \quad (4)$$

where i indicates the i-th reduction pass, σ_d is the pull/drawing stress, σ_b is the back-stress, α the die semi-angle, R_i and R_f are the wire initial and finish radii, L the bearing length and $\overline{\sigma}_{m_i}$ is the value of the average effective stress of the material within the die, calculated as follow:

$$\overline{\sigma}_{m_i} = \frac{\int_{\varepsilon_{0i}}^{\varepsilon_{fi}} \overline{\sigma} d\overline{\varepsilon}}{\int_{\varepsilon_{0i}}^{\varepsilon_{fi}} d\overline{\varepsilon}} = \frac{\int_{\varepsilon_{0i}}^{\varepsilon_{fi}} C\overline{\varepsilon}^n d\overline{\varepsilon}}{\overline{\varepsilon}_{f_i} - \overline{\varepsilon}_{0_i}} = \frac{C(\overline{\varepsilon}_{f_i}^{n+1} - \overline{\varepsilon}_{0_i}^{n+1})}{(n+1)(\overline{\varepsilon}_{f_i} - \overline{\varepsilon}_{0_i})}. \quad (5)$$

In Eq. 5, $\overline{\varepsilon}_{0_i}$ and $\overline{\varepsilon}_{f_i}$ are the effective strain of the material at the inlet and outlet of the i-th die, and C and n the strength and strain hardening coefficients of the ETP pure copper as reported in Eq. 8.

The term $f(\alpha)$ is a function of die semi-angle:

$$f(\alpha) = \frac{1}{\sin^2(\alpha)}\left[1 - \cos(\alpha)\sqrt{1 - \frac{11}{12}\sin^2(\alpha)} + \frac{1}{\sqrt{11{,}12}}\ln\left(\frac{1 + \sqrt{\frac{11}{12}}}{\sqrt{\frac{11}{12}}\cos(\alpha) + \sqrt{1 - \frac{11}{12}\sin^2(\alpha)}}\right)\right]. \quad (6)$$

The Capstan theorem (or theorem of Eytelwein) has been used to model the drive capstan between two consecutive passes of reduction [16],[17].

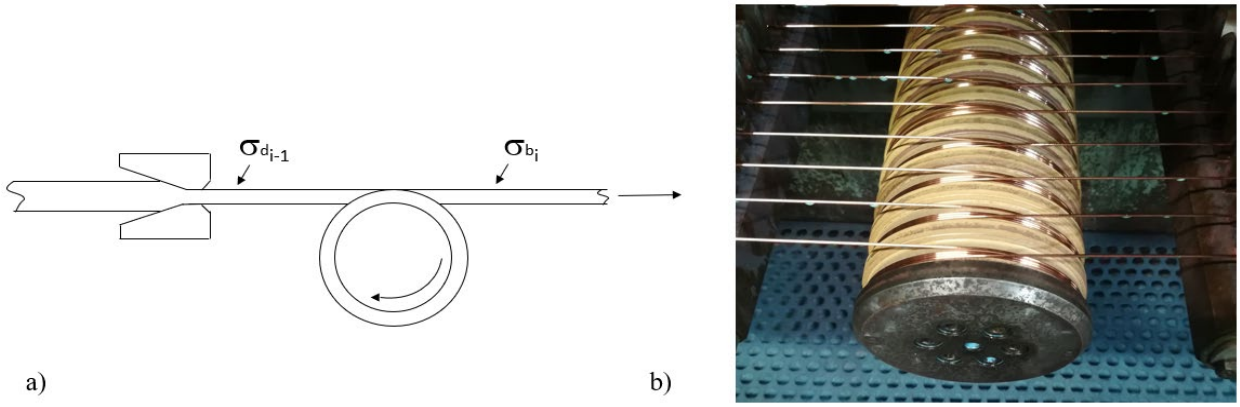

Fig. 3: a) Diagram of a capstan. Relation between drawing stress and back-stress; b) Picture of the capstan on industrial machine used in ICEL s.c.p.a.

The relation between drawing stress σ_d and the back-stress at the next die σ_b (Fig. 3) is expressed as follows:

$$\sigma_{b_i} = \sigma_{d_{i-1}} e^{-2\pi N \mu_c} , \tag{7}$$

where N is the number of windings of the wire around the capstan and μ_c is the friction coefficient between wire and capstan.

At the start of the drawing operation (step 1), σ_{d_1} is calculated without considering the contribution of the back-stress. From step 2 and for the next steps, σ_{b_i} is calculated considering the $\sigma_{d_{i-1}}$ contribution and then used to calculate σ_{d_i}.

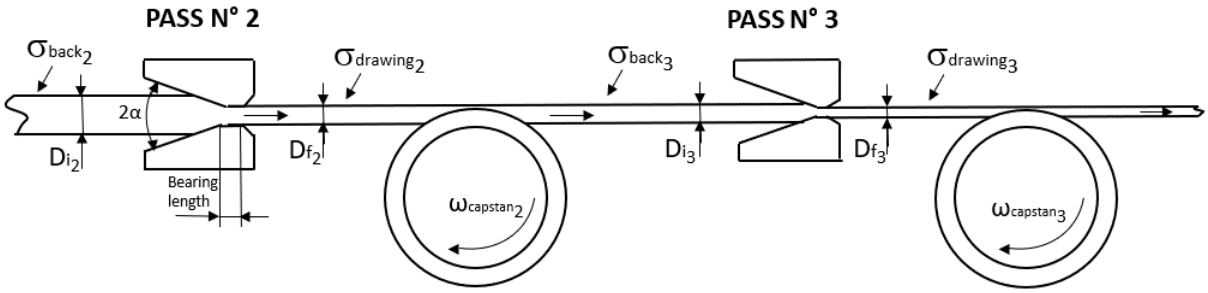

Fig. 4 Operation diagram of two consecutive drawing steps: pass number 2 and pass number 3

Material Characterization

Tensile tests on wires extracted at different reduction ratio were carried out to characterize ETP pure copper experimental flow stress data. After selected drawing passes, wire samples with a length of $L_0 = 200$ mm were extracted and tensile tests were coducted using a universal Instron 4301 testing machine. The tests were performed with an axial velocity of 0.1 mm/s. The maximum tensile true stress values collected during the tests are summarized in Fig. 5 with blue dots while the red curve was found in the literature [18] as output for the same material characterization. The red curve was modelled by Negroni et al. with the following equation:

$$\bar{\sigma} = C(\bar{\varepsilon})^n = 359(\bar{\varepsilon})^{0.149} . \tag{8}$$

Since a good correlation between the Negroni et al. material model and experimental tests was found Eq. 8 was used for Avitzur process modelling (Eqs. 4-6).

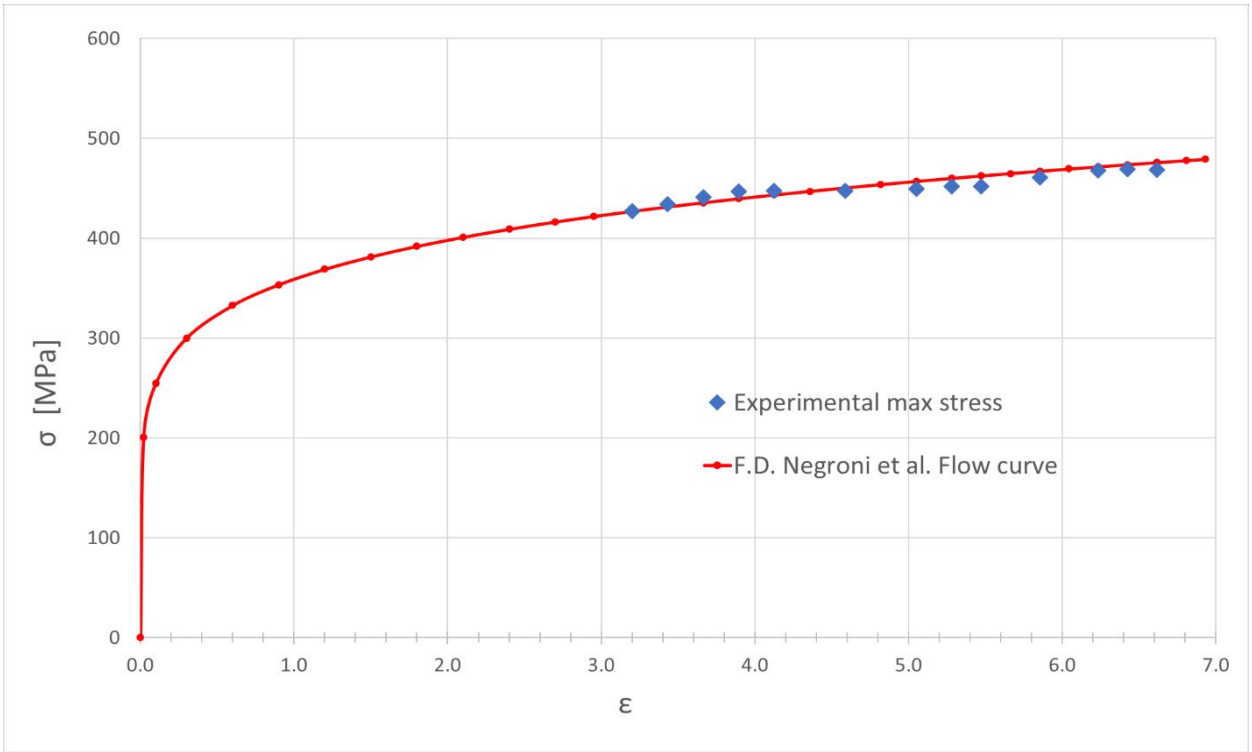

Fig. 5 Comparison between experimental values from tensile tests and the flow curve from F.D. Negroni et al. [18]

Results and Discussion

The drawing and back-stresses were compared with the yield stress step by step when different processing conditions were applied for both Machine 1 and Machine 2 (Fig. 6 and followings).

In these figures, the drawing stress is represented with a regular line and the back-stress with a dashed line. Moreover, green lines correspond to Machine 1 and red ones to Machine 2.

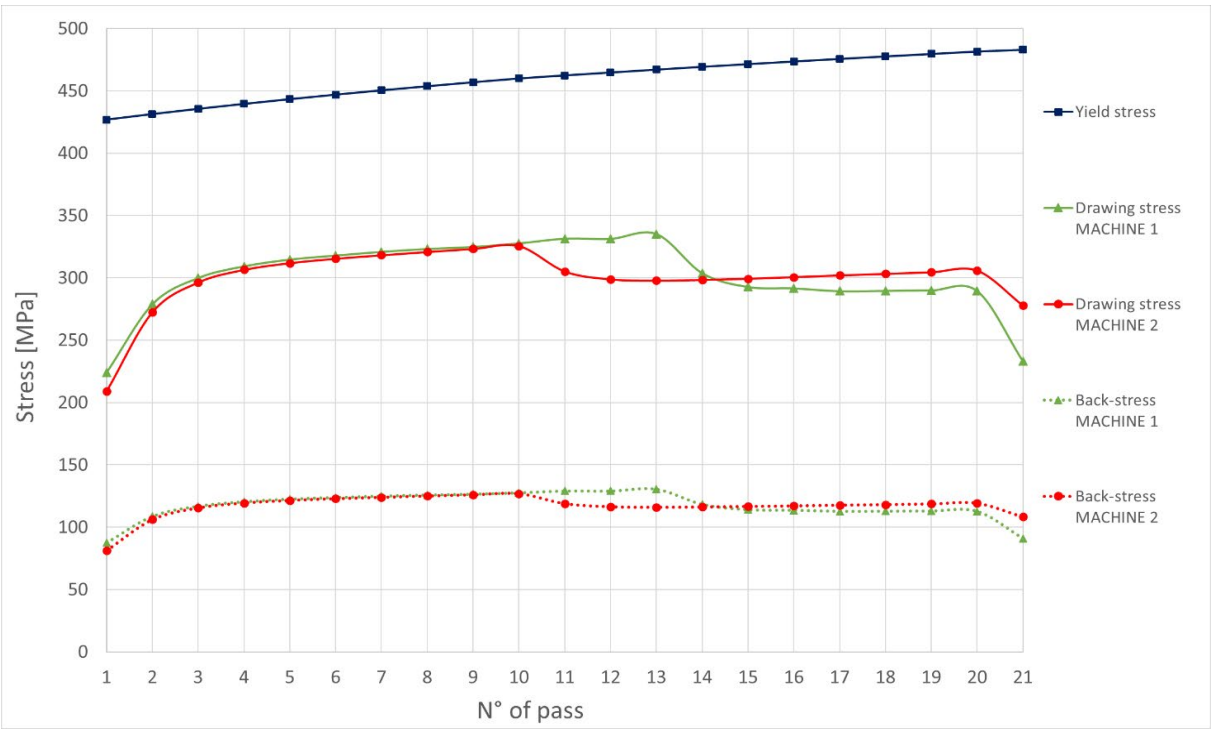

Fig. 6 Comparison between drawing stress and back-stress on Machine1 and Machine2 with coefficient of friction wire/dies and wire/capstans equal to μ=0.05 and the number of wire windings around each capstan equal to 3.

Fig. 6 shows the stresses when both friction coefficients between wire and die, and between wire and capstan are μ=0.05 [9],[13],[19], and the number of windings of the wire around all the capstans is 3. Clearly, the drawing stresses and back-stresses are always safely lower compared with the material yield stress although the two machine configurations produce different maximum drawing stresses: 340 MPa for Machine 1 at step 13 and 325 MPa for Machine 2 at step 10. It is also observable that, in Machine 1, a decrease of the stress occurs at pass 14 while, in Machine 2 it occurs at pass 11: these points correspond to the change of the machines' elongation ratio, which depends on the speed ratio of the gears' train moving the capstans, as previously described. In Machine 2, the wire is stressed more homogeneously along the steps while, in Machine 1, the wire is significantly stressed in the first steps (1-13) while, in the last steps (14-21) stress is significantly reduced. Regardless, the wires should always be safely produced by both machines since drawing stresses are always well below the wire yield stress. But it is also clear that, as the friction coefficient between wires and die increase (i.e. from 0.05 to 0.25) as found in [19], a considerable increase of the drawing stress acting on the wire may occur, as shown in Fig. 7. These friction coefficient values correspond to a lubrication regime that varies from an excellent lubrication with a thick film of lubricant to a limit lubrication with sticking between die and wire [19]. The changes in lubricant efficiency or in die wear may explains the different failure ratios of the two machines: in both machines these effects shift the drawing stress values close to the material resistance limit curve until pass n° 10; on Machine 1 the critical level is almost reached in steps from n° 11 to n° 13, making these steps the most critical, while on Machine 2 from pass n° 11 the stress values decrease to a safe level with respect to the material limit curves.

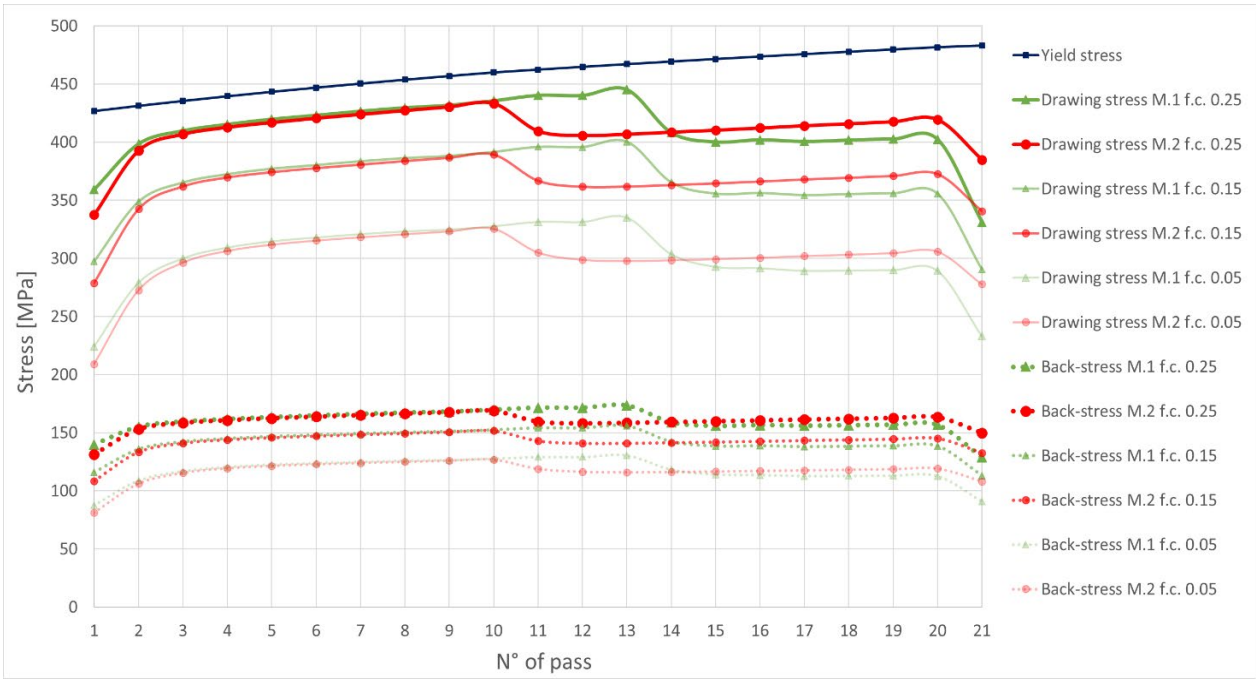

Fig. 7 Variation of the drawing stress and the back-stress with friction coefficient between wire and dies at each pass of reduction; friction between wire and capstan constant equal to μ_c=0.05; wire windings around capstan N=3.

In Fig. 8 the value of the drawing stress is calculated considering different friction coefficients between capstans and wire under the same friction coefficient μ=0.05 between wire and die. It must be noted that the friction coefficient between capstans and wire has an opposite effect on all the stresses compared with the friction coefficient between wire and die: an increase of the friction coefficient produce a relevant decrease of the drawing stress and of the back-stress at the inlet of each die. Similar trends can be plotted for Machine 2 as well.

Fig. 9 shows the drawing and back-stress behaviours considering different number of wire windings around the capstans. This parameter has a great impact on the management of process stresses. Increasing the number of windings from 2 to 3 and 4, the stresses decrease, because the back-stresses acting on the wire are reduced.

In Fig. 10, an optimization of the process was simulated on Machine 1 by acting on the number of windings of the wire around each capstan. The parameters set are shown in Table 2: the number of wire windings around the capstan has been set to 4 from pass 1 to pass 12; from pass number 13, when the elongation ratio of the machine decreases, the number of wire windings has been set to 3; in the last two passes the number of windings has been set to 2. It should be noted that a greater number of windings tends to increase the wearing of the wire, especially on the last steps where it becomes thinner. For this reason, the common practice is to set a decreasing number of windings from the inlet to the outlet of the machine. The proposed threading was tested on the machine, with good results on the frequency of wire failures; nevertheless, when a wire break occurs, it caused a longer machine downtimes, due to longer times to re-insert the machine and start-up. For this reason, its advantage within the industrial process is still under evaluation.

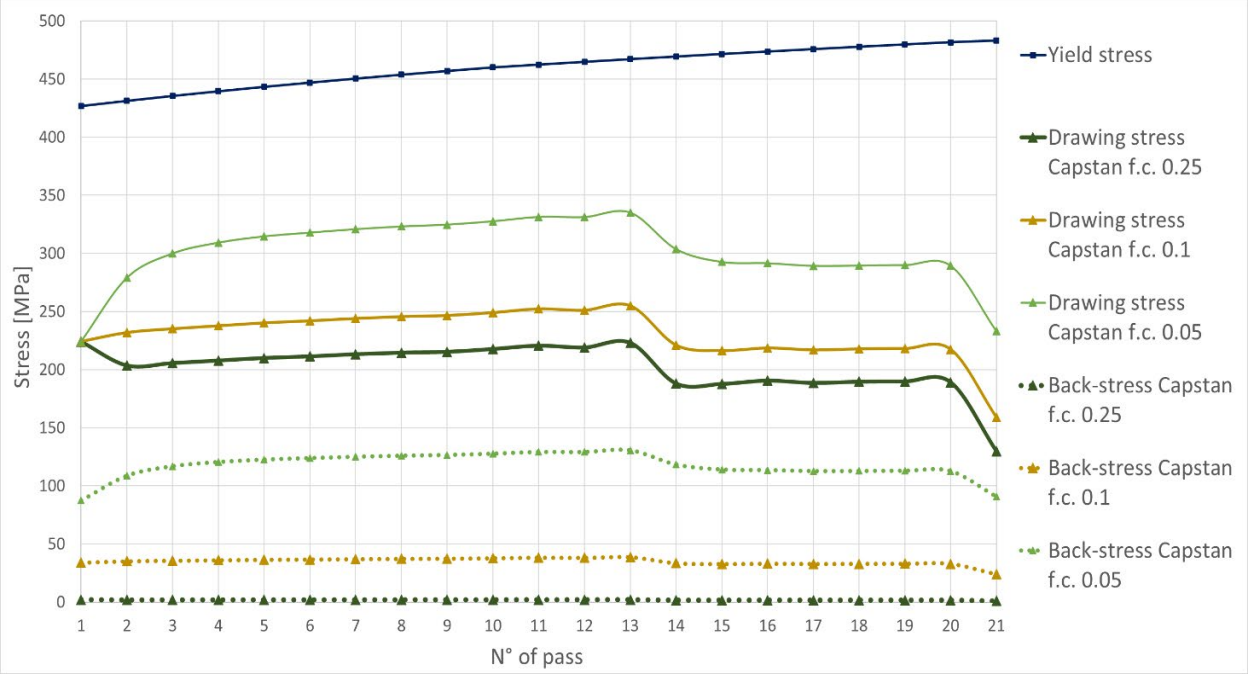

Fig. 8 Variation of the drawing stress and the back-stress with friction coefficient between wire and capstans at each pass of reduction on Machine1; friction between wire and die constant equal to μ_c=0.05; wire windings around capstan N=3.

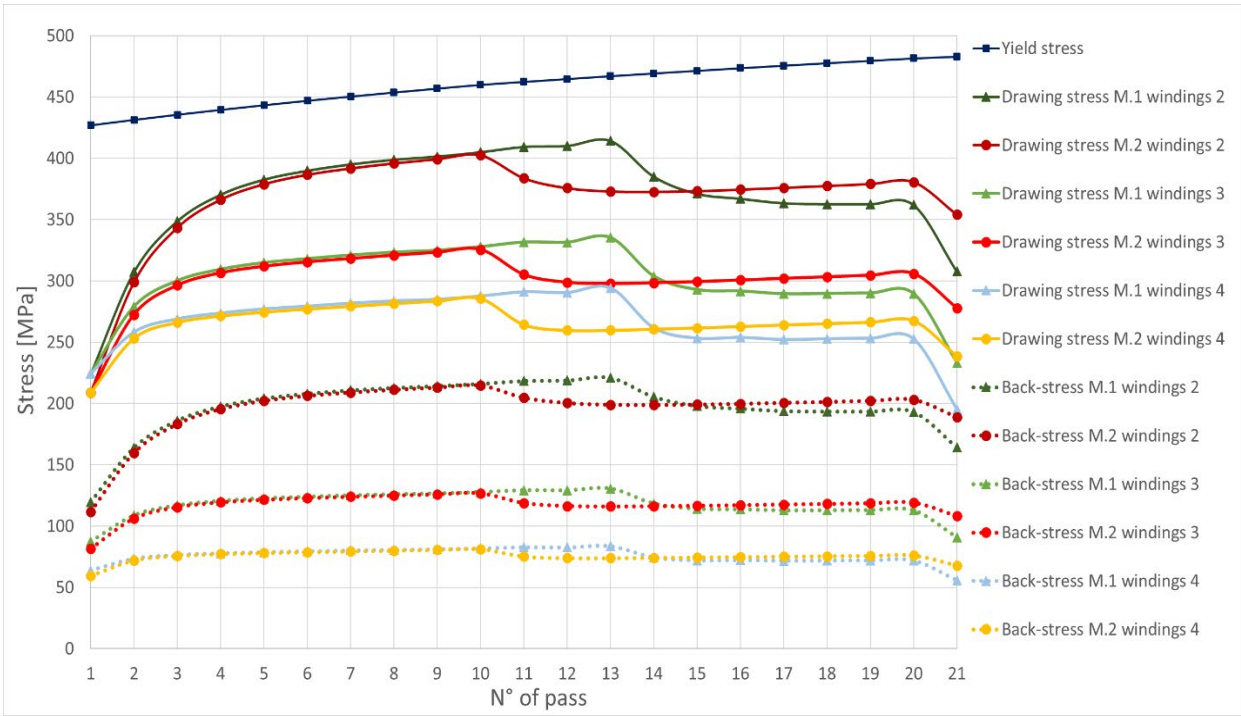

Fig. 9 Variation of the drawing stress and the back-stress with the number of windings of the wire around the capstans at each pass of reduction on Machine1 and Machine2; friction coefficient between wire/dies and wire/capstans equal to μ=0.05.

Table 2 Parameter values set on Machine1 to optimize the drawing stresses.

N° Pass	Diameter Initial [mm]	Diameter Final [mm]	Reduction ratio [%]	Die semi-angle [°]	Bearing length [mm]	Number of wire windings
1	1.83	1.592	24.3	9	0.398	**4**
2	1.592	1.417	20.8	9	0.354	**4**
3	1.417	1.261	20.8	9	0.315	**4**
4	1.261	1.122	20.8	9	0.281	**4**
5	1.122	0.998	20.9	9	0.250	**4**
6	0.998	0.888	20.8	9	0.222	**4**
7	0.888	0.790	20.9	9	0.198	**4**
8	0.790	0.703	20.8	9	0.176	**4**
9	0.703	0.626	20.7	9	0.157	**4**
10	0.626	0.557	20.8	9	0.139	**4**
11	0.557	0.495	21.0	9	0.124	**4**
12	0.495	0.441	20.6	9	0.110	**4**
13	0.441	0.392	21.0	9	0.098	**3**
14	0.392	0.359	16.1	9	0.090	**3**
15	0.359	0.329	16.0	9	0.082	**3**
16	0.329	0.301	16.3	9	0.075	**3**
17	0.301	0.276	15.9	9	0.069	**3**
18	0.276	0.253	16.0	9	0.063	**3**
19	0.253	0.232	15.9	9	0.058	**3**
20	0.232	0.213	15.7	9	0.053	**2**
21	0.213	0.205	7.4	9	0.051	**2**

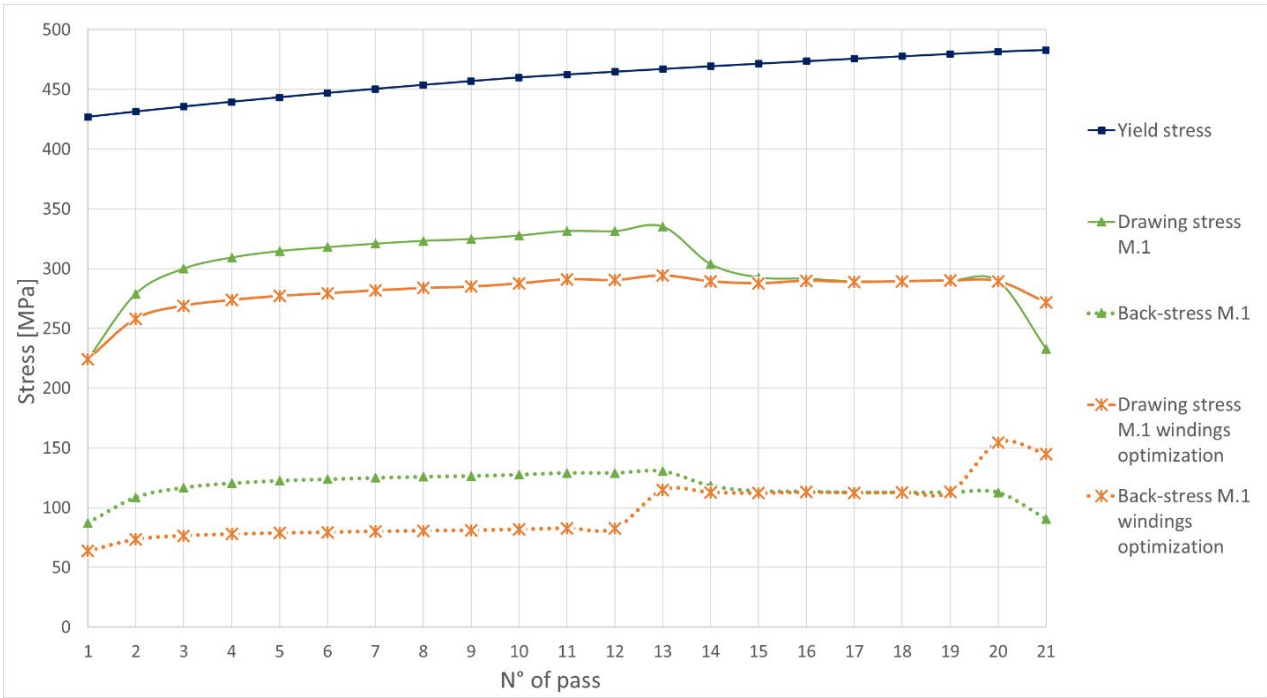

Fig. 10 Stress optimization by varying the number of the wire windings around the capstans in different pass of reduction on Machine1; friction coefficient between wire/dies and wire/capstans equal to μ=0.05.

Conclusions

In this work, the prediction model of the stresses acting on the material during the wire drawing process on multi-pass industrial machines was proposed and discussed.

The model was applied to the ETP Pure Copper (99.9% in weight) wire drawing using two industrial multi-pass machines, consisting of 21 passes of reduction with different elongation ratio.

Tensile tests were performed after each reduction pass to characterize the material plastic behaviour. The drawing stresses acting on the material were investigated and compared, step by step, to the material yield stress when different processing conditions were applied. The variation of the following process parameters was considered: friction coefficient between wire and die, friction coefficient between wire and capstan and the number of wire windings around the capstans.

The main outcomes of this work can be summarized as follows:

- If nominal processing conditions are used, the wire should not brake in relation to excessive drawing stresses.
- The different elongation ratios of the machines affect the homogeneity of the deformation. In Machine 2, the stress in the wire is more homogeneously while, in Machine 1, it is higher stressed in the first steps than in the last steps.
- The trend of the stresses is highlighted by varying the friction coefficients. It is evidenced that the friction coefficient between capstans and wire has an opposite effect on the stresses with respect to the friction coefficient between wire and die.
- A great influence of wire windings around the capstans on the wire stress behaviour is found. It is not possible to act on the wire reduction ratio at each step to reduce the tensions. Indeed, it is necessary that the mechanical elongation ratio of the machine remains lower than the elongation ratio of the wire. By acting on the number of windings it is possible to deform more homogeneously thus generating lower drawing stress values.

In the future, the effect of the capstans' speed (relative slip between wire and capstan) and the strain rate will be included in the modelling. Moreover, a study on the evolution of the friction coefficient of the lubricant over the working time is already planned.

References

[1] K. Osakada, History of plasticity and metal forming analysis, Journal of Materials Processing Technology 210(11) (2010) 1436-1454.

[2] K. Lange, Fundamentals of technical plasticity theory, in: Handbook of Metal Forming, first ed., Kurt Lange, Society of Manufacturing Engineers, 1985, pp: 99-132.

[3] K. Lange, Fundamentals of extrusion and drawing, in: Handbook of Metal Forming, first ed., Kurt Lange, Society of Manufacturing Engineers, 1985, pp: 461-487.

[4] J.G. Wistreich, The fundamentals of wire drawing, Metall Rev 3(10) (1958) 97-142.

[5] R. N. Wright, Basic Drawing Mechanics, in: Wire Technology-Process engineering and metallurgy, second ed., Butterworth-Heinemann, 2016, pp: 28-42.

[6] B. Avitzur, C. Narayan, Y.T. Chou, Upper-bound solutions for flow through conical converging dies, International Journal of Machine Tool Design and Research 22(3) (1982) 197-214.

[7] B. Avitzur, J.C. Choi, Compatibility of the upper-bound approach and the balance of forces for the treatment of metal-forming processes, Journal of Mechanical Working Technology 13(2) (1986) 141-150.

[8] U.S. Dixit, P.M. Dixit, An analysis of the steady-state wire drawing of strain-hardening materials, Journal of Materials Processing Technology 47(3–4) (1995) 201-229.

[9] G. Vega, A. Haddi, A. Imad, Investigation of process parameters effect on the copper-wire drawing, Materials & Design 30(8) (2009) 3308-3312.

[10] M. Tintelecan, I.M. Sas-Boca, D.A. Iluţiu-Varvara, The influence of the dies geometry on the drawing force for steel wires, Procedia Engineering 181 (2017) 193-199.

[11] A.I. Obi, A.K. Oyinlola, Frictional characteristics of fatty-based oils in wire drawing, Wear 194(1–2) (1996) 30-37.

[12] L. Lazzarotto, L. Dubar, A. Dubois, P. Ravassard, J. Oudin, Identification of Coulomb's friction coefficient in real contact conditions applied to a wire drawing process, Wear 211(1) (1997) 54-63.

[13] A. Haddi, A. Imad, G. Vega, Analysis of temperature and speed effects on the drawing stress for improving the wire drawing process, Materials & Design 32(8–9) (2011) 4310-4315.

[14] G.A.S. Martinez, W.L Qian, L.K. Kabayama, U. Prisco, Effect of process parameters in copper-wire drawing, Metals 10(105) (2020).

[15] J. Thimont, E. Felder, C. Bobadilla, P. Buessler, N. Persem, J.P. Vaubourg, Study of the wet multipass drawing process applied on high strength thin steel wires, AIP Conference Proceedings 1353 (2011) 467-472.

[16] R. N. Wright, Drawing Die and Pass Schedule in: DesignWire Technology-Process engineering and metallurgy, second ed., Butterworth-Heinemann, 2016, pp. 91-113.

[17] M. Herzog, Traction Force Increase caused by Deflection (Belt Friction), in: Copper wire drawing-Manufacuring of round copper wire for cable industry, first ed., Martin Herzog, 2019, pp. 186-187.

[18] F.D. Negroni, E.G. Thomsen, S. Kobayashi, A drawing modulus for multi-pass drawing, CIRP Annals 35(1) (1986) 181-183.

[19] R. N. Wright, Friction, Lubrication and Surface Quality in: DesignWire Technology-Process engineering and metallurgy, second ed., Butterworth-Heinemann, 2016, pp. 67-90.